Biophysical Chemistry 3 (1975) 215–225

KINETICS OF THE COOPERATIVE ASSOCIATION OF ACTIN TO ACTIN FILAMENTS†

Albrecht WEGNER and Juergen ENGEL
Department of Biophysical Chemistry, Biozentrum, Klingelbergstrasse 70, CH-4056 Basel, Switzerland

Received 6 February 1975; revised manuscript received 22 April 1975

The cooperative formation of actin filaments from monomers was followed by light scattering and electron microscopy. The results are well described by a simple model mechanism in which the growth and destruction of filaments occurs by stepwise addition or dissociation of protomers. All steps except the dimerisation step are assumed to have identical rate constants. These were found to be 5×10^3 $M^{-1} \cdot sec^{-1}$ and 3×10^{-2} sec^{-1} for the association and dissociation, respectively (at pH 7.5 and in the presence of 10^{-3} M calcium chloride). The equilibrium constant of elongation as obtained from the critical concentration is 1.7×10^5 M^{-1}. The corresponding equilibrium constant of dimerisation is about 10 million times smaller (cooperativity parameter $\sigma = 2 \times 10^{-7}$). This makes the nucleation extremely difficult and cooperativity very high. A best fit of the model to the experimental data is achieved when the destruction of a dimer is much faster than the addition of a third protomer (fast monomer–dimer pre-equilibrium). The size of the nucleus from which propagation becomes faster than dissociation is 3.

1. Introduction

The linear association of protein molecules to filamentous structures is a simple example of a self-assembly process. Such processes play an important role in biological organisation and it is of considerable interest to evaluate their thermodynamic and kinetic properties. It has been shown for the association of actin protomers to actin filaments [1,19] and for the formation of bacteria flagella from flagellin protomers [2] that association occurs only above a rather sharp critical monomer concentration. This proves the high cooperativity of these processes. Kinetic data have been evaluated for the actin [1,20] and flagellin [3] system mainly by viscosity and flow birefringence techniques. A model kinetic mechanism has been proposed for the association of actin and analyzed for the special case of irreversible polymerization [1]. A quantitative comparison of the theoretical prediction with experimental data, however, was hampered by the difficulty of deriving the polymer concentration from the data obtained with the techniques so far applied.

In the present work, the time course of the actin association was followed by light scattering. The experimental kinetic curves were analyzed in terms of a simple model mechanism without neglecting the dissociation steps.

2. Experimental procedure

2.1. Preparation of actin

Actin was prepared according to the method of Rees and Young [4] with the following alterations: The protein was chromatographed on Bio-Gel P 150 and protected against denaturation by modification with N-ethylmaleimide [5]. This modification does not affect the polymerization reaction [5].

2.2. Protein determination

Actin concentrations were determined photometrically using the biuret reaction [6]. The extinction coefficient was calculated from the known nitrogen con-

† Supported by Research Grant 3.1830.73 from the Schweizerischer Nationalfonds zur Foerderung der wissenschaftlichen Forschung.

tent, 16.1 g per 100 g protein, and from nitrogen determinations by the Kjeldahl method. The extinction coefficient at 540 nm was found to be 0.0613 cm^2/mg (Hitachi Spectrophotometer 101).

2.3. Polymerization conditions

Polymerization was carried out at 20° in a 10^{-3} M calcium-chloride solution, pH 7.5 (10^{-3} M triethanolamine–HCl buffer). Solutions contained 5×10^{-4} M ATP to prevent denaturation and 200 mg/l sodium azide to hinder bacterial growth. Under these conditions the polymerization reaction proceeded at a rate, which can be comfortably observed by means of light-scattering measurements, and the magnitude of the critical monomer concentration was such, that it could be accurately measured. Total actin concentrations were between 0.66 and 1.1 mg/ml (1.56×10^{-5} to 2.60×10^{-5} M). At higher concentrations the spontaneous formation of liquid crystals was observed.

2.4. Light scattering

Buffer and actin solutions were both centrifuged at 200 000 g for two hours to remove dust and polymers. In order to initiate aggregation by a sudden change in calcium-ion concentration 10 ml of actin solution were mixed with 5 ml of buffer in the light-scattering cell, the latter solution containing sufficient calcium chloride, so that the calcium-ion concentration in the final mixture was 10^{-3} M. Scattering curves were measured with a Cantow scattering photometer at 546 nm. The instrument was calibrated with benzene. The reduced scattering intensity at right angles to the incident beam was observed using unpolarized light, while the angular dependence of the scattering intensity was determined using a vertically polarized incident beam. The value of the molecular weight M_1 of monomeric actin was taken to be 42 300 [7], and the length of a subunit in the filament was assumed to be 28 Å [8,9]. On account of the very low salt and protein concentrations the solution was considered to have a refractive index negligibly different from that of water. The refractive increment was calculated according to the equation of Perlmann and Langsworth [10].

2.5. Electron microscopy

Grids were prepared according to the method of Huxley and Zubay [11] as modified by Hanson and Lowy [8], and by Kawamura and Maruyama [12]. Specimens were stained with 2% uranyl acetate and observed with a Zeiss EM 10 electron microscope at a voltage of 80 kV. The magnification was 2000–4000 and was calibrated with a carbon replica.

To determine the number average length, a number of electron micrographs taken from one grid were placed together so that the dimensions of the area examined were large compared with the lengths of the observed filaments. A rectangle was drawn on this composite picture far enough from its borders so that no filament crossed both, the rectangle and any edge of the composite picture. All those filaments which were more than half inside the rectangle were counted.

3. Theory

3.1. The model

An attempt will be made to fit the experimental results by the simple reaction scheme

$$2A \underset{k'_N}{\overset{k_N}{\rightleftharpoons}} A_2,\ A_2 + A \underset{k'}{\overset{k}{\rightleftharpoons}} A_3,\ \ldots,\ A_{i-1} + A \underset{k'}{\overset{k}{\rightleftharpoons}} A_i\,, \qquad (1)$$

where A stands for an actin molecule and in which the degree of association i is unlimited. Only four rate constants are introduced: k_N and k'_N for the formation and destruction of a dimer and k and k' for the binding and dissociation of protomers in elongation steps. Correspondingly only two parameters are needed for a description of the equilibrium behavior

$$K = k/k'\,, \quad \sigma K = k_N/k'_N\,, \qquad (2a,b)$$

where K is the equilibrium constant of elongation. The nucleation parameter σ is the ratio of the binding constants of dimerisation and propagation and is introduced in analogy to the treatment of other co-operative processes [13]. The nucleus is defined as the smallest aggregate for which elongation is faster than dissociation. In terms of our model the size of the nucleus is 2 if $k'_N < kc_1$ and it is 3 if $k'_N > kc_1$. The concentration of monomers is designated c_1 and c_i stands for the concentration of i-mers.

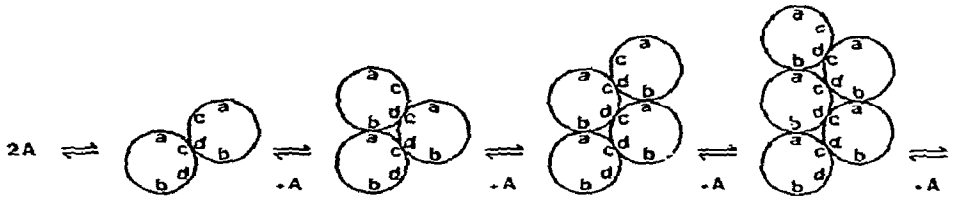

Fig. 1. Schematic representation of filament formation by mechanism (1). The designation of contact pattern is according to Oosawa and Kasai [1].

A basic assumption of the model is that all binding and dissociation steps which take place at the end of an actin filament have identical rate and equilibrium constants. This is certainly a very good approximation in view of the uniform structure of the filament. It is obvious that the first encounter of two actin molecules in the formation of a dimer is physically very different from all following steps and that different rate constants must be assigned to it. In the first step only one contact between the protomers is formed. In all other steps each molecule binds with two binding sites due to the double helical structure of the filament (see fig. 1). According to this picture the difference between the Gibbs free energies of elongation ΔG_E and that of nucleation ΔG_N is equal to the stabilizing energy which comes from the contact which forms only in elongation steps. Because of

$$\sigma = \exp\left[(\Delta G_E - \Delta G_N)/RT\right], \qquad (3)$$

and since the second contact probably contributes several kcal of binding energy a high cooperativity with $\sigma \ll 1$ is expected.

A limitation of the model is that only two different types of elementary steps are introduced and it is probably more realistic to assume that a number of different steps contribute to the formation of a nucleus with a critical size and that only after the nucleus is formed does further elongation proceed independently of i. Equilibrium calculations will not be altered by this extension of the model as long as the concentrations of species with small i are small. This will be particularly true at high cooperativity where long filaments are prefered [1,14]. The kinetics may, however, be influenced by the extension of the model, but the simple model is preferred over one with more parameters as long as it gives an adequate description of the experimental results.

In the model, all reactions between filaments are neglected. This assumption is justified as long as cooperativity is high. Even at the end of the reaction the concentration of monomeric actin will be much higher than the concentration of reactive ends at the filaments. Also the dissociation of a filament into two pieces involves the disruption of many more binding regions than the dissociation of an actin monomer from the end and is certainly much slower.

At this point it is worth mentioning that all constants in the scheme displayed in fig. 1 might be influenced by the ATP to ADP conversion which is involved in the actin association [15]. This, as well as a different association at the two ends of a filament, may further complicate the mechanism. It has been shown [16], however, that in the presence of an excess of ATP, model 1 (fig. 1) may be a good approximation. But it should be taken into account that K may contain a contribution of the ATP hydrolytic reaction which proceeds in a steady state under the experimental conditions.

3.2. Equilibrium

The equilibrium of actin association has been treated by Oosawa and Kasai [1] and by Winkelmair [14]. It was shown that at high cooperativity ($\sigma \ll 1$) association occurred only above a critical concentration of monomers $\bar{c}_1 = K^{-1}$ which remained constant in equilibrium with filaments. Furthermore, it was predicted that the equilibrium concentration of monomers was reached much faster than the equilibrium size distribution [17,25]. This justified the determination of $K = \bar{c}_1^{-1}$ from the end values of the progress curves of $c_p^* = c_{total} - c_1$ although the size distribution may still be quite different from the exponential true equilibrium distribution.

3.3. Kinetics

The aim of the kinetic treatment of the model mechanism is to predict the time dependence of the two experimentally observed quantities:

(1) the concentration of protomers incorporated in filaments

$$c_p^* = \sum_2^\infty i c_i = c_{total} - c_1 \; ; \tag{4}$$

(2) the molar concentration of filaments

$$c_p = \sum_2^\infty c_i \; . \tag{5}$$

Because of the above-mentioned difficulty in establishing defined equilibrium states, relaxation-type experiments which would permit a linearisation of the rate equations are not possible. The full set of differential equations must therefore be solved and c_p^* as well as c_p must be derived as a function of time and compared with the experimentally observed kinetics in order to evaluate the rate constants.

The rate equations are:

$$\begin{aligned} dc_2/dt &= k_N c_1^2 - k'_N c_2 - k c_1 c_2 + k' c_3 \; , \\ dc_i/dt &= k c_1 c_{i-1} - k' c_i - k c_1 c_i + k' c_{i+1} \; , \\ &(\infty > i > 3) \; . \end{aligned} \tag{6}$$

Integration of this complete set of differential equations may be performed by a numerical procedure. The differentials are replaced by finite increments which are chosen small enough so that no dependence on the stepwidth of the integration procedure is observed. Because of the long computer times needed this procedure was only applied as a check for the approximation which follows (see fig. 2). The number of rate equations of the set of rate equations (6) which were applied in the numerical integration was chosen to be twice as large as the average degree of association $\bar{i}$ which was reached for the parameters selected in the simulation. For these parameters the size distribution is such that polymers with $i > 2\bar{i}$ occur in completely negligible concentrations.

For the following approximation we can safely assume that after a short initial phase of the reaction a steady state will be established for filaments with a degree of association $i < q$. For the establishment of a steady state it is necessary that q is so small that the bulk of the polymers already formed has more than q subunits. Nevertheless q needs not to be a small number since in a cooperative association ($\sigma \ll 1$) long polymers are already formed in the beginning of the reaction.

With $dc_i/dt = 0$ we can express c_i by the concentrations of the q-mers and $(q+1)$-mers

$$c_i = c_q + (c_q - c_{q+1}) \sum_1^{q-i} s^{-j} \; , \tag{7}$$

where $s = Kc_1$. Hence it follows for the ratio of the dimer to trimer concentration:

$$\begin{aligned} c_2/c_3 &= 1 + (c_q - c_{q+1}) s^{2-q} \Big/ \left[c_q + (c_q - c_{q+1}) \sum_{j=1}^{q-3} s^{-j} \right] \\ &\approx 1 + (s-1) s^{2-q} (c_q - c_{q+1})/(s c_q - c_{q+1}) \; . \end{aligned} \tag{8}$$

The approximation in eq. (8) is valid if $s^{3-q} \ll 1$. Under our experimental conditions this is the case even for values of s near 1, since q may be a large number due to the formation of long filaments. If furthermore $c_{q+1} < s c_q$ eq. (8) reduces to $c_2/c_3 \approx 1$ for sufficiently large values of q.

The validity of the second assumption can only be proven by looking at the size distribution which develops during association. It has been demonstrated that maxima in the size distribution with $c_{i+1} > c_i$ may in fact develop. The size distributions are sharpest if $s = kc_1/k' \to \infty$, this is when back reactions can be neglected. Under this condition and for a constant number of nuclei a Poisson distribution is predicted [23], which is the sharpest size distribution which can be expected for any linear polymerization reaction which is not regulated by a template [27]. A size distribution which is more relevant to our case in which nucleation is much slower than elongation has been calculated theoretically by Dostal and Mark [24] but again irreversibility was assumed. Here the size distribution is much more broad at the side of small i and c_{i+1}/c_i is about 1 at any point even if we look at the distribution near completion of the reaction. In the beginning of the reaction a flat distribution with $c_i \approx c_{i+1}$ and in particular $c_2 \approx c_3$ is observed for

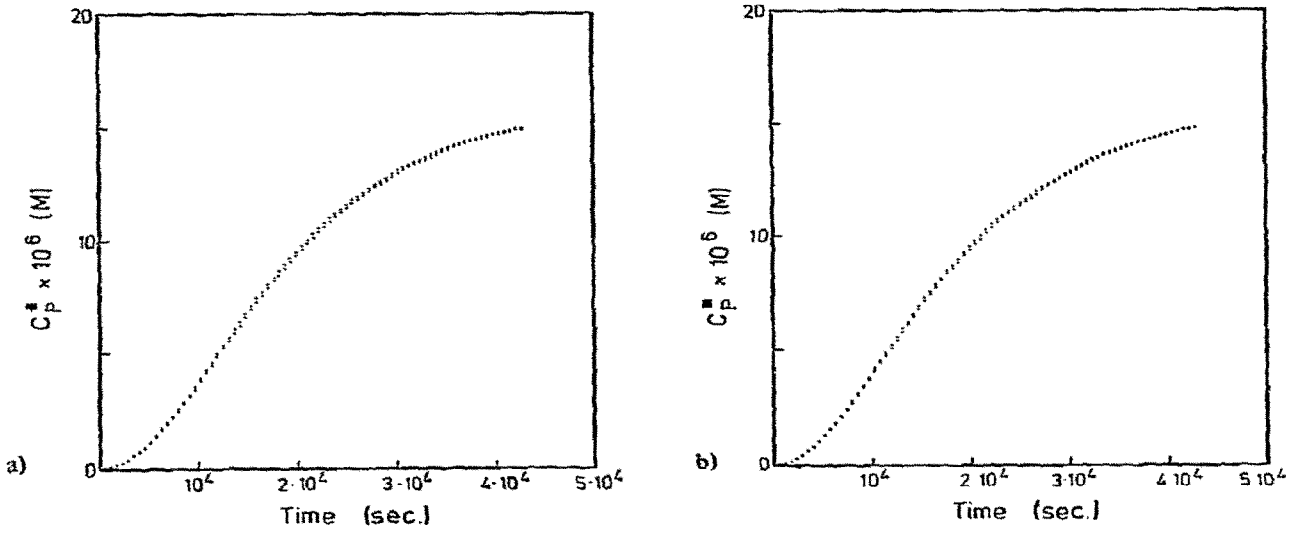

Fig. 2. Comparison of the time dependence of the concentration of protomers which are incorporated in filaments c_p^* as calculated by numerical integration of eq. (6) (upper curves in a and b) and by the approximate eqs. (10) and (12) (lower curves in a and b). The following parameters were used: (a) $c_{total} = 2.2 \times 10^{-5}$ M, $k = 1.7 \times 10^5$ M^{-1}, $k_N = 0.31 \times 10^{-2}$ $M^{-1} \cdot sec^{-1}$, $k'_N = k' = 3 \times 10^{-2}$ sec^{-1}, $k = 5.1 \times 10^3$ $M^{-1} \cdot sec^{-1}$. (b) $c_{total} = 2.2 \times 10^{-5}$ M, $k = 1.7 \times 10^5$ M^{-1}, $\sigma = 2.2 \times 10^{-7}$, $k = 5.1 \times 10^3$ $M^{-1} \cdot sec^{-1}$. The assumption of a fast monomer–dimer equilibrium $k_N \gg kc_1 - k'$ is made.

small degrees of association. The introduction of reversibility leads to an even larger flattening of the distribution at the side corresponding to small chain lengths, as the numerical analysis described at the beginning of this section has shown. It may be postulated that the ratio c_{i+1}/c_i can only approach but never reach or exceed s at any point and any time if the reaction is started from monomers only. If $c_{i+1}/c_i = s$ would be reached, c_i would convert at the same rate into c_{i+1} as c_{i+1} is converted into c_i. This resembles the case of linear diffusion which would lead to a lowering of the gradient.

With $c_2 \approx c_3$ it is possible to express c_2 in terms of c_1 only:

$$c_2 \approx k_N c_1^2/(k'_N + kc_1 - k') . \tag{9}$$

The rate of the change of polymer concentration is

$$dc_p/dt = k_N c_1^2 - k'_N c_2$$

$$\approx [k_N(kc_1 - k')c_1^2]/(k'_N + kc_1 - k') . \tag{10}$$

The rate by which protomers are incorporated into filaments is

$$dc_p^*/dt = dc_2/dt + kc_1 \sum_3^\infty c_i - k' \sum_4^\infty c_i . \tag{11}$$

According to the steady-state condition dc_2/dt is zero. Since c_3 and c_4 are small compared with the sum of the concentrations of the other polymers the two sums in eq. (11) are nearly equal to c_p and eq. (11) becomes

$$dc_p^*/dt \approx (kc_1 - k')c_p . \tag{12}$$

Numerical stepwise integration of the two differential equations (10) and (12) yields the desired time dependence of c_p^*.

Proof for the validity of this approximation comes from the excellent agreement with the full solution obtained by numerical integration (fig. 2). This comparison was performed for two widely different sets of parameters.

As it is found by inserting the integrated eq. (10) in eq. (12), the time dependence of c_p^* is fully determined by a set of three independent parameters: e.g. k'_N/k', $k_N k$, and $k_N k'$. If K is known from the critical concentration, it is possible to obtain k'_N/k' and $k_N k$

from a fit of the theoretical dependence to the experimental data.

It is, however, not possible to evaluate any of the rate constants separately from measurements of c_p^* alone. This can be achieved only when c_p is also measured.

Of particular importance is the special case $k'_N \gg kc_1 - k'$ which means that a fast pre-equilibrium is established between c_1 and c_2. Eq. (10) then reduces to $dc_p/dt = \sigma K(kc_1 - k')c_1^2$. For our experimental conditions with $s < 5$ the same result is obtained for $k'_N/k' \gg 1$. In the case of fast pre-equilibrium the time dependence of c_p^* which is obtained by stepwise integration of eq. (12) with the simplified eq. (10) is uniquely determined by the parameters $k\sqrt{\sigma K}$ and $k'\sqrt{\sigma K}$ and with the known K by $k\sqrt{\sigma}$.

3.4. Evaluation of c_p^* from light-scattering data

For a polydisperse solution of rods with lengths $L_i > \lambda^*$ and diameters much less than λ^* the following equation for the Rayleigh ratio $R(\theta)$ was derived [18]

$$K_L C/R(\theta) = (2/\pi^2)\left(\sum_i M_i w_i/L_i^2\right)/\left(\sum_i M_i w_i/L_i\right)^2 + 1/\left(\lambda^*\pi \sum_i M_i w_i/L_i\right) + \ldots . \quad (13)$$

M_i is the molecular weight of the ith component, w_i are the corresponding weight fractions and $C = c_p^* M_1$ is the weight concentration of polymers.

$$K_L = 2\pi^2 n^2 (dn/dC)^2/(N_L \lambda^4) \qquad \lambda^* = \lambda'/(4\pi \sin \tfrac{1}{2}\theta), \quad (14a,b)$$

where λ and λ' are the wavelengths of the incident light and of the light in solvent, respectively, n is the refractive index, dn/dC is the refractive-index increment, N_L is Avogadro's number and θ is the angle under which the scattered light is observed relative to the direction of the incident beam. The mass–length ratio is the same for all actin filaments. Furthermore, the length L_i of an actin rod with polymerization degree i is equal to i times the length l of a subunit in the filament. With the help of these relationships, and by replacing each weight fraction by the respective molecular concentration c_i it follows that

$$K_L C/R(\theta) = (2/\pi^2)\left(\sum c_i\right)/C + l/(\lambda^* \pi M_1). \quad (15)$$

At large observation angles the first term can be neglected to yield

$$c_p^* = R(\theta)\, l/(\pi \lambda^* K_L M_1^2). \quad (16)$$

This equation is applicable because small filaments which do not meet the conditions under which it was derived are formed only in very small concentrations. This is proven by the electron-microscopic results and also by the light-scattering results itself: already a very short period after starting the polymerization, the dependence of $1/R(\theta)$ on $\sin \frac{1}{2}\theta$ predicted by eq. (15) was established. For molecules with dimensions smaller than λ^* a dependence on $\sin^2 \frac{1}{2}\theta$ is expected. In addition it may be shown that the scattering of monomeric actin is so small compared to that of the polymers that no correction must be applied for it in eq. (16).

4. Results

4.1. Critical monomer concentration

This value was obtained by the same method as applied by Oosawa et al. [19]. Fig. 3 shows a plot of $c_{p\,final}^*$ versus c_{total}. The $c_{p\,final}^*$ values have been obtained from the end values of the curves shown in fig. 5. These values are no true equilibrium values (see subsect. 3.2), but since the monomer–polymer equilibrium is essentially established, K^{-1} may be obtained from an extrapolation of these data to $c_p^* = 0$. A value of $K = 1.7 \times 10^5\ M^{-1}$ is found.

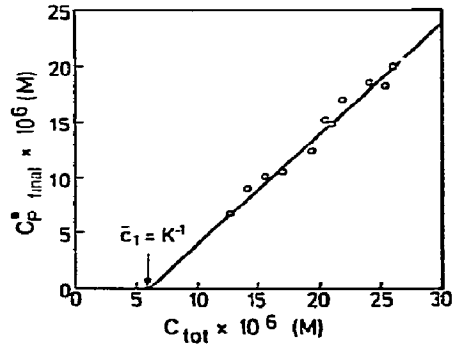

Fig. 3. Evaluation of the critical monomer concentration $\bar{c}_1 = K^{-1}$ from a plot of the end values of the kinetic curves (see fig. 5) versus the total actin concentration.

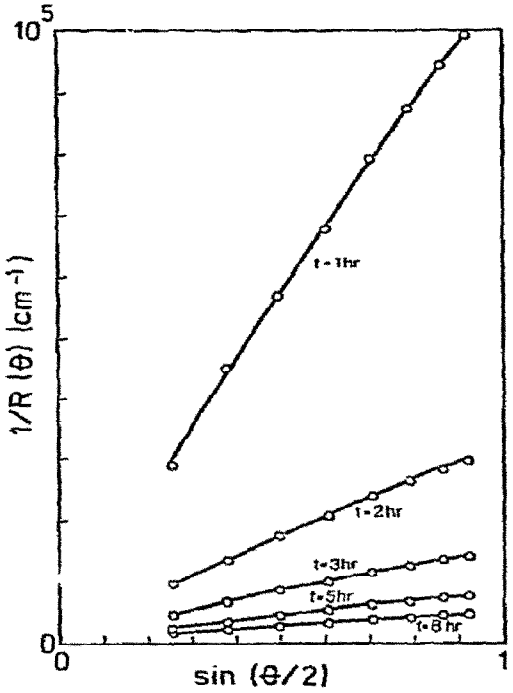

Fig. 4. Reciprocal reduced light-scattering intensity versus $\sin\frac{1}{2}\theta$ during the course of actin association. The total concentration was 22×10^{-6} M.

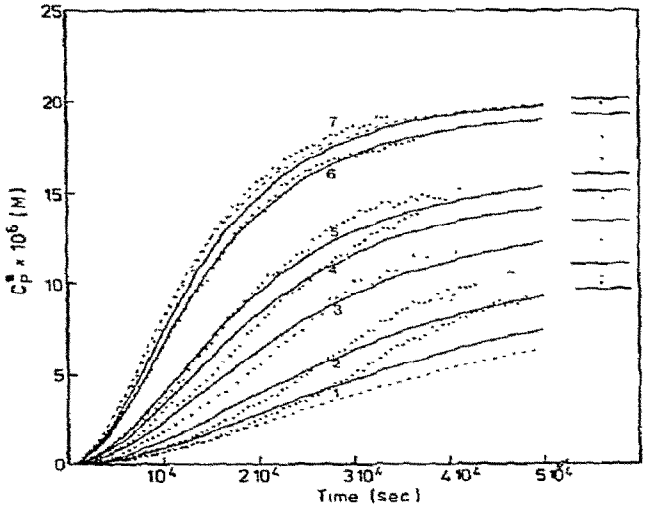

Fig. 5. Dotted lines: Time dependence of c_p^* for the total actin concentration 1: 15.6×10^{-6} M, 2: 17.0×10^{-6} M, 3: 19.4×10^{-6} M, 4: 21.0×10^{-6} M, 5: 22.0×10^{-6} M, 6: 25.3×10^{-6} M, 7: 26.0×10^{-6} M. At the right side of the figure the end values obtained after 1 to 3 d are shown. Drawn-out curves: Theoretical curves obtained for $K = 1.7 \times 10^5$ M^{-1} and $k\sqrt{\sigma} = 2.4$ M$^{-1}\cdot$sec^{-1} with the assumption of a fast monomer–dimer equilibrium (see table 1). Broken lines: Theoretical curves obtained for the highest and the lowest concentrations (26.0×10^{-6} M and 15.6×10^{-6} M) with the assumption of a fast monomer–trimer equilibrium. The parameters are adjusted to fit the kinetic curve at the high concentration.

4.2. Time dependence of c_p^*

Fig. 4 shows light-scattering curves measured after different times. Already after 1 h in which a very small fraction of polymers is formed the light-scattering curves show the $\sin\frac{1}{2}\theta$ dependence predicted for long rods (see subsect. 3.4). Fig. 5 shows the experimental kinetic data of c_p^* as calculated from the light-scattering data with eq. (16).

To fit these data by the time dependence of c_p^* predicted by the model the set of parameters leading to the smallest standard error of the monomer concentration was sought.

The standard error is defined as:

$$\Delta c_1 = \left(\sum_1^N (c_{1f} - c_{1m})^2/N\right)^{1/2},$$

where c_{1f} and c_{1m} are the calculated and measured monomer concentrations, respectively, and N is the number of experimental points. As the calculated equilibrium constant of propagation $K = 1.7 \times 10^5$ M^{-1} was known from the critical concentration the two parameters which were varied in the fitting procedure were k'_N/k' and $k_N k$. When the special case of fast monomer–dimer equilibrium was assumed only $k\sqrt{\sigma}$ was adjusted.

Table 1 shows that the best agreement is obtained by fitting the experimental data with the assumption of a fast monomer–dimer pre-equilibrium. This case appears in the concentration range of our measurements, when the rate constant k'_N for the dimer dissociation is by a factor of ten or more greater than that of the depolymerisation k'.

The fitting was also carried out for each total concentration separately. In table 1, the relative differences of the kinetic parameters determined by the above two methods are shown. The relative difference is defined as

$$\Delta p = (p - P)/P,$$

Table 1
Parameters and standard deviations corresponding to the theoretical curves which represent the best fit to the experimental data shown in fig. 5 ($K = 1.7 \times 10^5$ M)

k'_N/k'	$k_N k$ ($M^{-2} \cdot sec^{-2}$)	Standard error (M^{-2})	Δp at different total concentrations (μM)						
			15.6	17.0	19.4	21.0	22.0	25.3	26.0
1	16	0.46×10^{-12}	−0.10	−0.10	−0.12	−0.07	+0.01	+0.04	+0.15
2	20	0.36×10^{-12}	−0.07	−0.07	−0.11	−0.07	+0.01	+0.03	+0.12
5	33	0.29×10^{-12}	−0.01	−0.03	−0.09	−0.06	+0.02	+0.01	+0.09
10	56	0.27×10^{-12}	−0.01	−0.01	−0.08	−0.06	+0.01	−0.01	+0.07
fast monomer–dimer pre-equilibrium	$k\sqrt{\sigma} \approx$ 2.4 $M^{-1} \cdot sec^{-1}$	0.26×10^{-12}	+0.06	+0.02	−0.08	−0.05	+0.02	−0.02	+0.05

where P is one of the three (or two) parameters obtained by a simultaneous fitting to all measured curves and p is the corresponding parameter obtained by a best fit to a single curve. For small ratios of k'_N to k', p differs systematically from P: the measured curves at low total concentrations yield smaller p values than those at higher concentrations. When k'_N/k' approaches 10 and for the case of fast pre-equilibrium these systematic differences disappear.

It is demonstrated that the assumption of a nuclear size larger than 3 will lead to a higher concentration dependence than experimentally observed. For this end the theoretical progress curves (dashed curves in fig. 5) were calculated for the highest and lowest concentrations with the assumption of a fast monomer–trimer equilibrium. This corresponds to a nucleus which consists of 4 actin protomers. The curve-fitting parameters are adjusted to fit the kinetic curve at the high concentration. The curve for the low concentration is calculated with the same set of parameters.

4.3. Determination of the molar concentration of filaments c_p

This polymer concentration was determined in an actin solution (22.0 μM) after a polymerization time of 11.5 h. After this time, at which further polymerization is very slow, a sample was applied to a grid of the electron microscope and the number average filament length was determined. The lengths of the actin filaments were measured in three regions on a grid. The number averages of the lengths were 2.5, 2.5, 2.8 μM for these regions. The total number of actin filaments considered was 586. With a length of 28 Å per subunit a number average 923 for the degree of polymerization is calculated. According to the light-scattering measurements obtained at the same time that the grids were prepared, c_p^* was 1.44×10^{-5} M. Hence the molar polymer concentration was 1.56×10^{-8} M.

By integration of eq. (10), inserting the parameters obtained from light-scattering experiments, numerical values for k_N, k'_N, k, k' and σ were obtained (table 2). Of course for the case of fast monomer–dimer pre-equilibrium no values for the rate constants of dimerisation can be evaluated and only the equilibrium constant of nucleation σK is obtained.

5. Discussion

The best fit of the experimental data with the model mechanism proposed in subsect. 3.1 is obtained with the assumption of a fast monomer–dimer pre-equilibrium.

Systematic deviations between experimental and theoretical curves lessen when increasing ratios of k'_N/k' are assumed. The improvement, as judged from the standard error, is large when k'_N/k' rises from 1 to 5, it is small at ratios higher than 5 and no further improvement is achieved at ratios larger than 10. Under our experimental conditions the ratio of the rate of foreward propagation to reverse propagation $s = kc_1/k'$ is smaller than 5. This means that $k'_N \leqslant k'(s-1)$ for $k'_N/k' \leqslant 4$. The more k'_N/k' exceeds the value of 4 the better is the condition for fast pre-equilibrium $k'_N \gg kc_1 - k' = k'(s-1)$ fulfilled. This

Table 2
Rate constants obtained by fitting procedure for different ratios of k'_N/k'

k'_N/k'	k_N ($M^{-1} \cdot sec^{-1}$)	k'_N (sec^{-1})	k ($M^{-1} \cdot sec^{-1}$)	k' (sec^{-1})	$\sigma \times K$ (M^{-1})	σ
1	0.31×10^{-2}	3.0×10^{-2}	5.1×10^{3}	3.0×10^{-2}	0.100	6×10^{-7}
2	0.39×10^{-2}	6.0×10^{-2}	5.2×10^{3}	3.1×10^{-2}	0.064	3.8×10^{-7}
5	0.66×10^{-2}	1.5×10^{-1}	5.1×10^{3}	3.0×10^{-2}	0.044	2.6×10^{-7}
10	0.11×10^{-1}	3.0×10^{-1}	5.1×10^{3}	3.0×10^{-2}	0.037	2.2×10^{-7}
fast monomer–dimer pre-equilibrium	–	–	5.1×10^{3}	3.0×10^{-2}	0.037	2.2×10^{-7}

proves that at least for not too high s values the dissociation of a dimer occurs much faster than the addition of one more actin molecule to form a trimer. The first stable nucleus in the sense that growth is faster than dissociation is the trimer. This size of the nucleus was established earlier by Kasai et al. [20] from the concentration dependence of initial rates of polymer formation. If our model mechanism would be extended by the assumption of more than one nucleation step in the fast pre-equilibrium it would predict a much higher concentration dependence than observed.

There is some analogy with the kinetics of the formation of the double helix from single stranded oligonucleic acids [21]. In this instance the dissociation of base pairs was found to be faster in the first three steps than in all following steps. On the other hand, comparing the cooperative association of actin with the highly cooperative coil–α-helix conversion of polypeptides we find a striking difference. For the latter system it was found [22] that the rate constant for the formation of the first helical segment is much slower than that of propagation steps, whereas all reverse-rate constants are essentially the same. The explanation is that for this system the reversal of the first step and of the propagation steps are very similar processes. Both involve the opening of one hydrogen bond and about the same number of other stabilizing interactions. For actin, however, in the dissociation of a dimer only one protein–protein contact has to be broken whereas the dissociation of an actin molecule from the end of a filament involves the disruption of the whole set of interactions (at least two pairs of protein binding sites) which stabilize the filamentary structure. For the double-helix–coil conversion a similar explanation is offered: in the reversion of the first steps either no or less stacking interactions are broken.

The theoretical kinetic curves predicted by the model with the inclusion of a fast monomer–dimer pre-equilibrium fit the experimental data reasonably well (fig. 5). In particular, the overall concentration dependence is very well represented. At lower concentrations some systematic deviations between the predicted and experimentally observed sigmoidicities and polymer concentrations c_p^* are found. The high observed values of c_p^* at the later stage of polymerization could be a result of a slow breakage of filaments, which leads to an acceleration of the consumption of monomers. Oosawa and Kasai [1] have formulated a more complex mechanism which accounts for the formation of single stranded linear aggregates. These authors have limited their kinetic analysis of the model to the special case of irreversible propagation steps ($kc_1 \gg k'$). For this special situation their theoretical results are exactly identical with those derived in the present paper for a much simpler model. This shows that no distinction between the two models can be made on the basis of such kinetic data. The irreversible case is certainly a poor approximation if kc_1/k' approaches unity.

As it has been pointed out in subsect. 3.3 the fit of the c_p^* versus time curves alone does not yield the rate constants and the supplementary determination of the molar concentration of filaments c_p for at least one point in the kinetics is much less accurate. It was done via a determination of the average length of the filaments determined by electron microscopy. This technique may involve a number of serious systematic errors. The most severe one may be a change of the

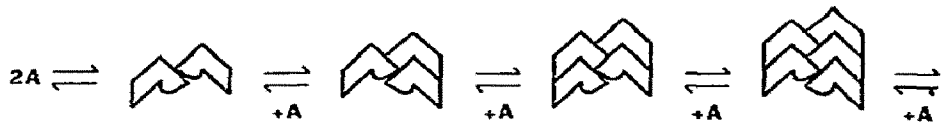

Fig. 6. Schematic drawing of a possible induced fit mechanism in actin association.

degree of association during preparation of the specimens for electron microscopy. We have selected a sample which was already in the slow saturation phase of its kinetics in order to avoid part of this problem. A breakage of filaments during adsorption on the grids can, however, not be excluded. This effect would lead to too high c_p values and to too low rate constants k and k'. There is an indication that large filaments may be preferentially broken during adsorption. We observed an almost exponential size distribution of filaments, although for this time and under the experimental conditions applied according to Oosawa [25] and to own unpublished calculations, larger polymers should pre-dominate. In view of these limitations of the electron-microscopic technique the rate constants as well as the cooperativity parameter σ represented in table 2 are probably not very accurate but they should reflect the right order of magnitude. A decrease in the average length by a factor x would yield a σ which is x^2 times too high, and also x times too small rate constants k and k'.

The value of σ is unexpectedly low. This means that the free energy of dimer formation is 9.2 kcal less favourable than that of a propagation step. With the binding constant of propagation it follows that dimers are extremely unstable. The free energy of their formation amounts to almost +2 kcal and the corresponding binding constant is 3×10^{-2} M^{-1}. In the framework of our simple picture this would mean that the first interaction between two actin molecules cd in fig. 1 contributes 2 kcal of unfavourable interaction energy. In order to make the free energy of the second step −7.2 kcal ($K = 1.7 \times 10^5$), the second contact (a–b in fig. 1) should contribute −9.2 kcal. It is not likely that in the filament such large differences between the two contact regions persist since this leads to a dissociation of the filament into two strands. More likely is an internal rearrangement via conformational changes as sketched in fig. 6. Therefore the initial bad contact in the dimer would be rendered into a stable one by the addition of the third protomer. This idea is not in contradiction to our first formulation of the model mechanism (eq. (1)).

The rate constant for the addition of an actin molecule to the end of a filament $k \approx 5 \times 10^3$ M$^{-1} \cdot$ sec^{-1} is small compared to other interactions between proteins. For example, the overall rate constant for the binding of pancreatic trypsin inhibitor (Kunitz) to α chymotrypsin was found to be 10^6 M$^{-1} \cdot$ sec^{-1} [26]. This process consists of a fast (probably diffusion-controlled) bi-molecular first step and a slower mono-molecular second step. It is highly probable that a similar two-step mechanism holds true also for the binding steps in the actin association. Compared to the above inhibitor–enzyme interaction the proper encounter of an actin monomer with its binding site on the filament may be more difficult because of the necessity to establish at least two pairs of contacts. In addition, we have to keep in mind that the not very well understood splitting of ATP to ADP may be a rate-limiting step in this process.

The values which are reported in table 2 for a given ratio of $k'_N/k = 10$ are consistent with the experimental data but they only represent lower limits. For the more likely case when $k'_N/k \gg 10$ the kinetics are exclusively determined by σK, k and k'. The rate constants of the fast pre-equilibrium can therefore not be extracted from the data.

Acknowledgements

We thank Miss Doris Dreher in the Department of Microbiology for the expert help with the electron microscope and Miss Bea Rutschmann for her technical assistance.

References

[1] F. Oosawa and M. Kasai, J. Mol. Biol. 4 (1962) 10.
[2] S. Asakura, Advan. Biophys. 1 (1970) 99.

[3] S. Asakura, J. Mol. Biol. 35 (1968) 237.
[4] M. Rees and M. Young, J. Biol. Chem. 242 (1967) 4449.
[5] C.J. Lusty, H. Fasold, Biochemistry 8 (1969) 2933.
[6] A. Gomall, C. Bardawill and M. David, J. Biol. Chem. 177 (1949) 751.
[7] M. Elzinga, J.H. Collins, W.M. Kuehl and R.S. Adelstein, Proc. Nat. Acad. Sci. USA 70 (1973) 2687.
[8] J. Hanson and J. Lowy, J. Mol. Biol. 6 (1973) 46.
[9] C.C. Selby and R.S. Bear, J. Biophys. Biochem. Cytol. 2 (1956) 71.
[10] G. Perlmann and L. Langsworth, J. Am. Chem. Soc. 70 (1948) 2719.
[11] H. Huxley and G. Zubay, J. Mol. Biol. 2 (1960) 10.
[12] J.M. Kawamura and K. Maruyama, J. Biochem. 67 (1970) 437.
[13] J. Engel and G. Schwarz, Angew. Chem. Internat. Edit. 9 (1970) 389.
[14] D. Winkelmair, Arch. Biochem. Biophys. 147 (1971) 509.
[15] F.B. Straub and G. Feuer, Biochim. Biophys. Acta 4 (1950) 455.
[16] F. Oosawa and S. Higashi, Progr. Theor. Biol. 1 (1967) 79.
[17] A. Miyake and W.H. Stockmayer, Makromolek. Chem. 88 (1965) 90.
[18] E.F. Casassa, J. Chem. Phys. 23 (1955) 596.
[19] F. Oosawa, S. Asakura, K. Hotta, N. Imai and T. Ooi, J. Polymer Sci. 37 (1959) 323.
[20] M. Kasai, S. Asakura and F. Oosawa, Biochim. Biophys. Acta 57 (1960) 22.
[21] D. Pörschke and M. Eigen, J. Mol. Biol. 62 (1971) 361.
[22] G. Schwarz and J. Engel, Angew. Chem. 11 (1972) 568.
[23] P.J. Flory, J. Amer. Chem. Soc. 62 (1940) 1561.
[24] H. Dostal and H. Mark, Z. physik. Chem. B29 (1935) 299.
[25] F. Oosawa, J. Theor. Biol. 27 (1970) 69.
[26] U. Quast. J. Engel, H. Heumann, G. Krause and E. Steffen, Biochemistry 13 (1974) 2512
[27] M. Szwarc, Carbanions, Living Polymers and Electron Transfer Processes (Interscience Publishers, New York, 1968).